Supplemental Material:

The CaMKK2/CaMKIV relay is an essential regulator of hepatic cancer

Fumin Lin[1], Kathrina L. Marcelo[1], Kimal Rajapakshe[1], Cristian Coarfa[1], Adam Dean[1], Nathaniel Wilganowski[3,4], Holly Robinson[3,4], Eva Sevick[3,4], Karl-Dimiter Bissig[1,2,6], Lauren C. Goldie[5,6,7], Anthony R. Means[1,2,*] and Brian York[1,2,*,††]

[1] Department of Molecular and Cellular Biology, Baylor College of Medicine, Houston, TX
[2] Dan L. Duncan Cancer Center, Baylor College of Medicine, Houston, TX
[3] The University of Texas Health Science Center, Houston, TX
[4] Center for Molecular Imaging, Institute of Molecular Medicine, Houston, TX
[5] Department of Pediatrics, Baylor College of Medicine, Houston, TX
[6] Center for Cell and Gene Therapy, Baylor College of Medicine, Houston, TX
[7] USDA/ARS Children's Nutrition Research Center, Baylor College of Medicine, Houston, TX

MATERIALS AND METHODS

Liver Tissue Samples

Tumorous and non-tumorous liver tissues were obtained from 22 patients who underwent surgery for clinical diagnosis of HCC. Protein lysates were generated by standard protocols. All institutional policies for protection of patient rights and identity have been followed.

Additionally, immunohistochemistry staining for CaMKK2 was performed on liver cancer biopsies from patients with hepatocellular neoplasia (HCN), hepatoblastoma (HB), hepatocellular carcinoma (HCC). The HCN sample was from a male patient with an activating NRAS mutation (somatic, Q61K), but no reported underlying etiology. The HCC sample was from a male patient with mitochondrial DNA depletion syndrome with a mutation in MPV17. Liver sectioning revealed micronodular cirrhosis with multiple nodules of hepatocellular cancer. Finally, the HB sample originated from a female with no known risk factors or genetic abnormalities. Histology revealed mixed epithelial components (90% fetal, 5% embryonal hepatoblastoma, 5% mesenchymal).

Cell Culture

HepG2, Hepa1-6, SK-Hep1 and Hep3B cells were obtained from ATCC and cultured under standard conditions. TPH cells were generated from the liver tissues of WT C57BL/6 mice approximately 16 months after DEN injection. PHM1 cells were a kind gift from Dr. Kathryn O'Donnell of UT Southwestern Medical School with permission from Scott Lowe.

Reagents

Anti-CaMKK antibody (pan-KK) was from BD Biosciences. Anti-P-mTOR, anti-mTOR, anti-P-PDK1, anti-P-S6K T389, anti-P-S6 S240/244, anti-P-S6 S235/236, anti-S6, anti-P-4EBP1, anti-P-AMPKα T172, anti-AMPKα and anti-HSP90 antibodies were from Cell Signaling Technology. Anti-P-CaMKI T177 and anti-P-CaMKIV T200 antibodies were from Santa Cruz Biotechnology. Anti-CaMKI antibody was from Abcam. Anti-CaMKIV and anti-β-actin antibodies were from Sigma. Anti-CaMKK2 antibody for IHC was from Atlas Antibodies. Anti-puromycin antibody was from KeraFAST. All siRNAs and scrambled siRNAs were from Life Technologies. shRNA against *CaMKK2* was obtained from Open Biosystems, including negative control pLKO (TRCN0000241923), shRNA3142 (TRCN0000028815), shRNA3143 (TRCN0000028761) and shRNA3145 (TRCN0000028776).

Animal Care

All mouse experiments were performed in accordance with the Animal Care Research Committee at Baylor College of Medicine. The generation of *CaMKK2*$^{-/-}$ mice has been described. All mice were bred and maintained on a pure C57BL6/J background. Mice were maintained in a temperature controlled (23^{o}C) facility with a 12 h light/dark cycle. Mice were fed 2920X Teklad Global rodent chow *ad libitum* with free access to food and water. Nude mice (NU/J) were purchased from Jackson Laboratories.

Plasmid and siRNA Transfection

Plasmids were transfected into liver cancer cells using Lipofectamine 2000 (Life Technologies) per the manufacturer's instruction. siRNA was transfected using RNAiMAX Lipofectamine (Life Technologies) per the manufacturer's instruction.

shRNA Lentivirus Generation and Infection

shRNA vectors were transfected into 293T cells with lentiviral packaging plasmids using Lipofectamine 2000 (Life Technologies) per the manufacturer's instruction. Either 24 or 48 h after transfection, cell medium was harvested, filtered and centrifuged at 25,000 rpm at 4^{o}C for 3 h to collect virus. PHM1 cells were infected with virus containing sham shRNA pLKO vector, or *CaMKK2* (3142, 3143 or 3145 clones) shRNA vector using polybrene per the manufacturer's instruction. Following infection, cells were screened with puromycin (2 μg/ml). Selected stable cell lines were maintained in media with 1 μg/ml puromycin.

Cell Cycle Analysis

For analysis of cell cycle distribution of PHM1 cells based on cellular DNA and RNA content, single cell suspensions were stained with 10 μg/mL Hoechst 33342 (Sigma-Aldrich) at 37ºC for 45 min, followed by

addition of 1 µg/ml pyronin Y (Sigma-Aldrich) for another 15 min. Single cell suspensions were washed and resuspended in HBSS/10% FBS followed by flow cytometry using an LSRII (BD Biosciences) analyzer.

Immunohistochemistry

For paraffin embedding, freshly-dissected liver and tumor biopsies were fixed in 10% neutral buffered formalin overnight at 4ºC. Tissues were washed in PBS several times, stored in 70% ethanol at 4ºC until embedded in paraffin and sectioned at 5 µm.

For colorimetric immunohistochemical staining, paraffin-embedded sections were de-paraffinized and rehydrated using standard methods. Antigen retrieval was performed by incubating sections in 1X Target Retrieval Solution (Dako, Carpinteria, CA) for 10 min at 95°C. The slides were allowed to cool for 10 min at RT, and then washed twice with PBS for 5 min. Several blocking steps were performed by incubating sections in the following solutions: (1) endogenous immunoperoxidase blocking using 3% H_2O_2 solution for 10 min at RT, (2) non-specific blocking using NDS blocking media for 1 h at RT, and (3) endogenous biotin blocking using Streptavidin-Biotin Blocking Kit (Vector Laboratories, Burlingame, CA), per the manufacturer's specifications. Tissue sections were then incubated overnight at 4°C with primary antibodies diluted to 1:100 in 0.2X NDS blocking medium in TBS with 0.1% Tween-20. After several washes with PBS, sections were incubated for 1 h at RT with biotinylated species-specific secondary antibodies diluted to 1:1000 in 0.2X NDS blocking medium. After washing with PBS, sections were incubated for 30 min at RT with Pierce High Sensitivity Streptavidin-Labeled Horse Radish Peroxidase (Thermo Fisher Scientific Inc., Rockford, IL) diluted at 1:1000 in PBS. Colorimetric detection of bound antigens was performed using ImmPACT DAB detection reagent (Vector Laboratories) per the manufacturer's specifications. Tissue sections were counterstained with hematoxylin, dehydrated and cleared using standard methods, and mounted using VectaMount® permanent mounting media (Vector Laboratories, Burlingame, CA). Images were captured with a Zeiss AxioObserver microscope fitted with an AxioCam ICc3 color camera, using Zeiss AxioVision version 4.8.2.0 software (Carl Zeiss MicroImaging, Thornwood, NY).

Gene Expression Profiling

For gene expression profiling of mouse liver cells, total RNA was extracted using Trizol (Invitrogen) and purified with the RNeasy Mini Kit (Qiagen) following the manufacturer's instructions. RNA was reverse transcribed and the microarray hybridization was performed using the Illumina Gene Expression Mouse WG-6 v2.0 Expression BeadChip Kit at the Laboratory for Translational Genomics at Baylor College of Medicine. Microarray scanned images were imported to Illumina® GenomeStudio for data quality control and the transcriptome profile data were quantile-normalized by the Bioconductor Lumi package (46). Differences in gene expression between si*CAMKK2* and the siControl sample groups were inferred utilizing the Bioconductor limma package (47) ($p<0.05$) and imposing a fold change exceeding 1.25x, using the R statistical system. Hierarchical clustering and heatmaps were also generated using the R statistical system.

Gene Set Enrichment Analysis

Gene Set Enrichment Analysis (GSEA) was carried out using the GSEA software package (48) to assess the degree of similarity among the studied gene signatures. For the si*CAMKK2* transcriptome response, all genes were ranked by the fold-change between the si*CAMKK2* and the siControl sample groups. From the previously published HCC progression gene signature (24, 25), we utilized separately the down-regulated genes and the up-regulated genes. Normalized Enrichment Score (NES) and adjusted q-values were computed utilizing the GSEA method, based on 1000 random permutations of the ranked genes. We further determined enriched pathways using the gene set collections at the Molecular Signature Database (MSigDB, http://www.broadinstitute.org/gsea/msigdb/) using a hypergeometric distribution ($p<0.05$).

HCC Tumor Progression Gene Signature

We utilized a public Hepatocellular Carcinoma (HCC) dataset (24, 25), GSE14520. For downstream analysis, the signature was partitioned into up- and down-regulated genes.

Survival Analysis

Survival analysis for individual genes or gene signatures was performed by sorting all the patient samples based on the individual expression or signature scores. The survival or disease-free survival Kaplan-Meier

plots were generated using “survival” package in the R statistical system. The significance was determined by log-rank test (weights 0 or 4, respectively).

Comparison of siCamkk2 Activity Score vs Tumor Progression Score in HCC Patient Cohorts

We downloaded gene expression datasets from a previously reported human HCC specimen cohort (24, 25). For each dataset, we replaced the gene expression of each gene with the z-score with respect to the normal liver gene signature available in each cohort. For both the si*CAMKK2* and the HCC tumor progression transcriptome fingerprints, we computed the sum z-score for each sample by adding the z-score for up-regulated genes and subtracting for down-regulated genes, as described previously (49). Finally, for each pair of signatures we plotted the cumulative z-scores on the X- and Y-axis, and computed the Pearson Correlation Coefficient R and associated p-value using the R statistical system.

Proliferation Assay

Liver cancer cells were seeded at 2 x 10^4/mL/well into a 12-well plate. Cell number was determined using a Countess automated cell counter each day for 5 days.

Tumorigenicity in Nude Mice

Six-week-old male nude mice were subcutaneously injected with 2x10^6/100µl PHM1 cells with control shRNA into the left flank and 2x10^6/100µL PHM1 cells with *CaMKK2* shRNA into the right flank. The tumor volume was calculated as 0.5 x length x $width^2$ 2X/week for 6 weeks. For STO-609 treatment, 2x10^6/100µl control PHM1 cells were subcutaneously injected into nude mice. After tumors reached 3mm^3, mice were divided into two groups with comparable tumor volume. Each group received vehicle (10% DMSO in PBS) or STO-609 by i.p. injection (30µg/kg body weight) 2X/week for 4-weeks. At the end of the experiment, GFP fluorescence was measured using a Biospectrum AC Imaging System (UVP, LLC).

References for Supplemental Materials & Methods

1. Du P, Kibbe WA, & Lin SM (2008) lumi: a pipeline for processing Illumina microarray. *Bioinformatics* 24(13):1547-1548
2. Smyth GK (2004) Linear models and empirical bayes methods for assessing differential expression in microarray experiments. *Stat Appl Genet Mol Bio*l 3: Article 3.
3. Subramanian A, et al. (2005) Gene set enrichment analysis: a knowledge-based approach for interpreting genome-wide expression profiles. *Proc Natl Acad Sci U S A* 102(43):15545-15550.
4. Roessler S, et al. (2010) A unique metastasis gene signature enables prediction of tumor relapse in early-stage hepatocellular carcinoma patients. *Cancer Res* 70(24):10202-10212.
5. Roessler S, et al. (2012) Integrative genomic identification of genes on 8p associated with hepatocellular carcinoma progression and patient survival. *Gastroenterology* 142(4):957-966 e912.
6. Taylor BS, et al. (2010) Integrative genomic profiling of human prostate cancer. *Cancer Cell* 18(1):11-22

Supplemental Figure 1

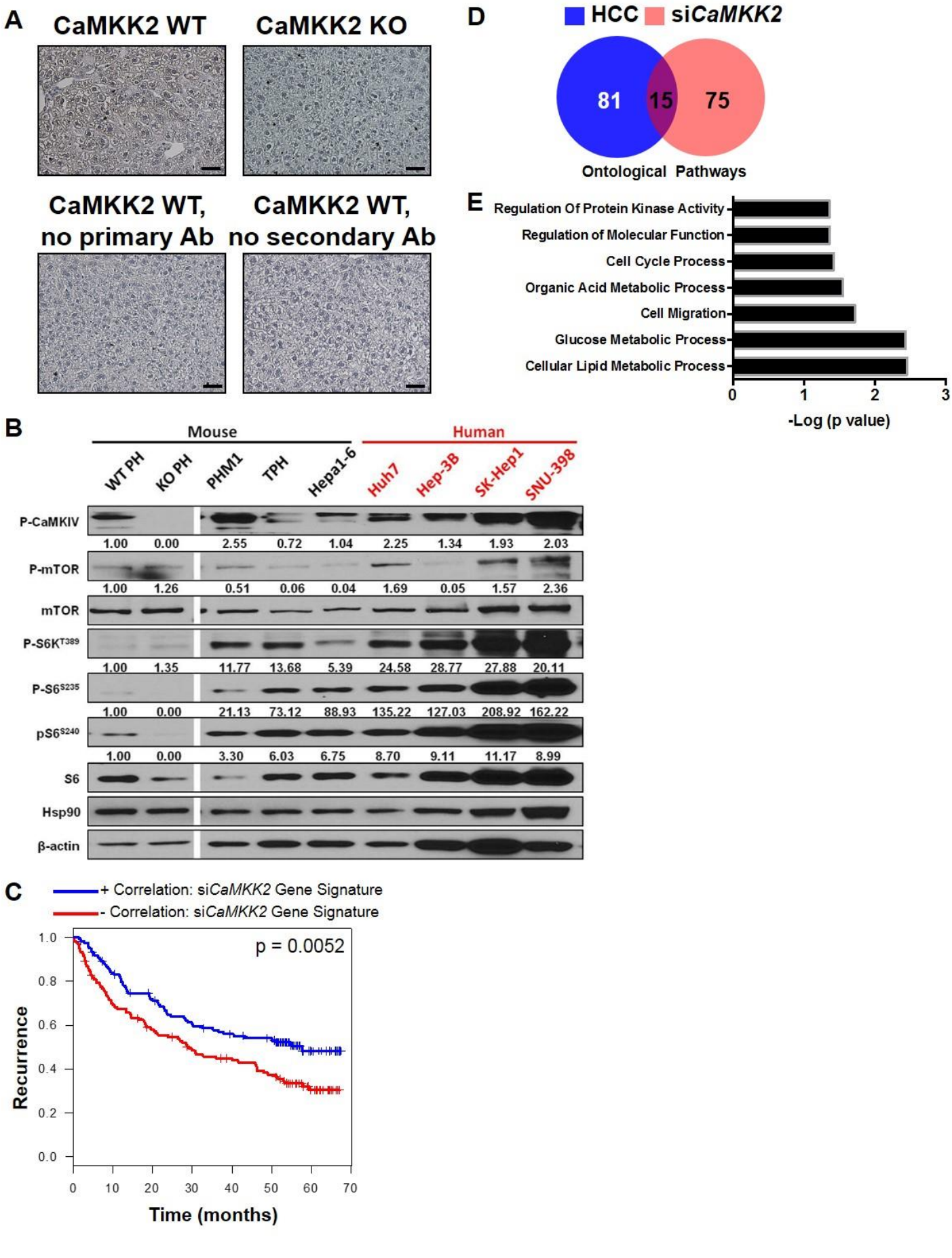

Supplemental Figure 1. CaMKK2 is upregulated in liver cancer biopsies and cell lines.
(A) Immunohistochemical staining of paraffin-embedded liver sections from wild type (positive control) and CaMKK2$^{-/-}$ (KO, negative control) mice. Additional negative IHC controls, which include CaMKK2$^{+/+}$ liver sections stained without either primary (anti-CaMKK2) antibody or secondary (biotin-conjugated anti-rabbit) antibody, are also shown. Scale bars = 10 µm.
(B) Immunoblot of CaMKK2 substrates and components of the mTOR pathway in primary hepatocytes and various mouse and human liver cancer cell lines, corresponding to **Figure 1D**.
(C) Kaplan-Meier recurrence and survival curves of liver cancer patients (n = 247) comparing low *CaMKK2* + *CaMK4* expression (blue lines) with high *CaMKK2* + *CaMK4* expression (red lines).
(D) Venn diagram showing the overlap of gene ontologies for genes changed in the human HCC dataset (blue) versus knockdown of *CaMKK2* by siRNA (red).
(E) Graphical summary of overlapping ontological pathways determined from the human HCC dataset and si*CaMKK2* gene signatures.

Supplemental Figure 2

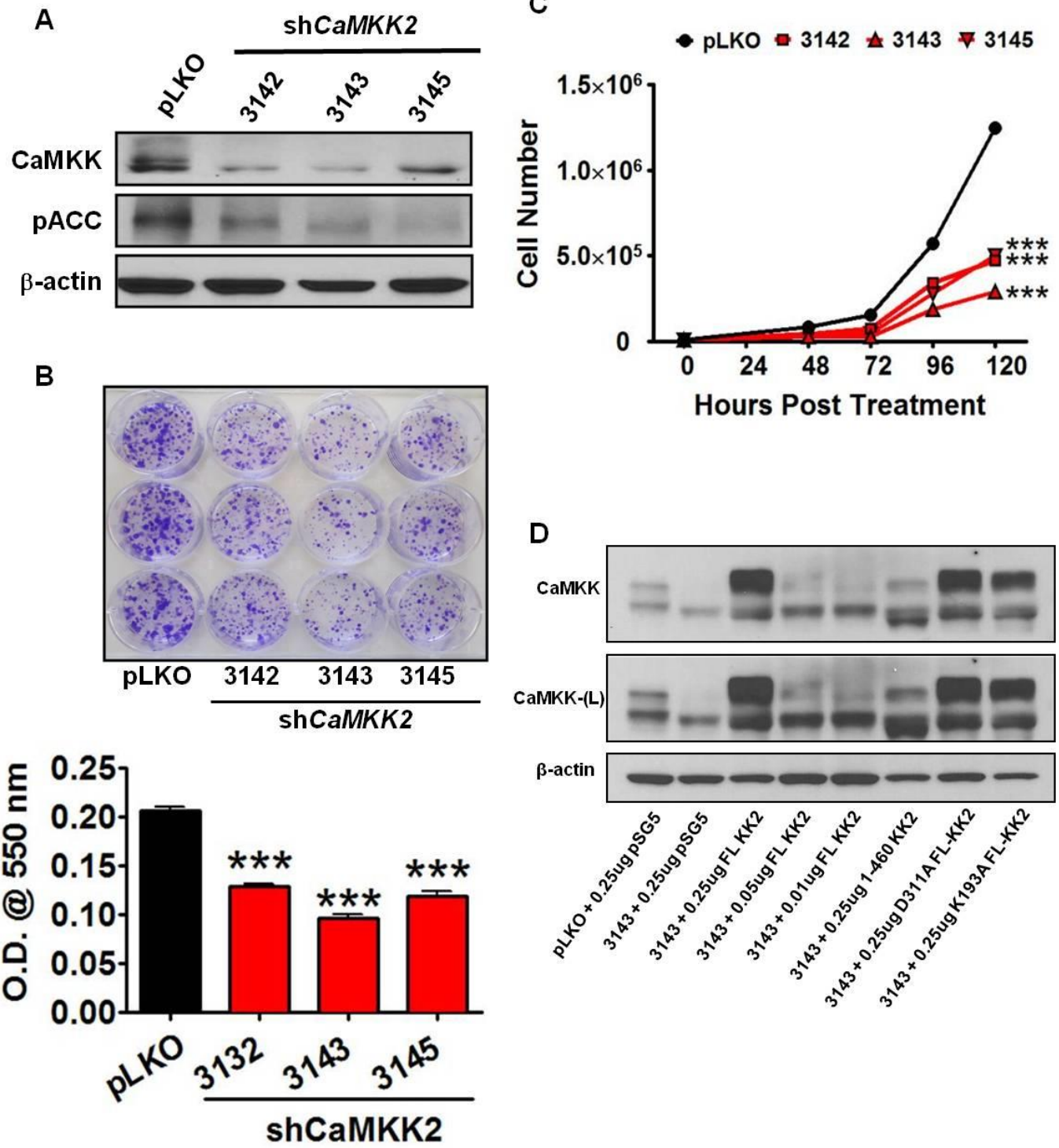

Supplemental Figure 2. Loss of CaMKK2 activity attenuates the liver cancer cell growth *in vitro*.
(A) Immunoblot verifying the knock down efficiency of *CaMKK2* by shRNA in PHM1 cells. Phospho-ACC is used as a proxy to monitor the inhibitory effects of CaMKK2 on AMPK signaling.
(B) Crystal violet staining of colony formation assays in PHM1 control (pLKO) or three independent stable knockdown clones using *CaMKK2* shRNA (Clone IDs: 3142, 3413, 3415).
(C) Time course proliferation assay of PHM1 cells infected with control (pLKO) or *CaMKK2* shRNA (Clone IDs: 3142, 3413, 3415).
(D) Corresponding to **Figure 2D**, immunoblot to verify the ectopic expression of various CaMKK2 constructs in control (pLKO) or stable *CaMKK2* shRNA (Clone ID: 3145) knockdown PHM1 cells.
Data are graphed as the mean ± s.e.m. Shown are the representative replicates of at least three independent experiments. ***p<0.001.

Supplemental Figure 3

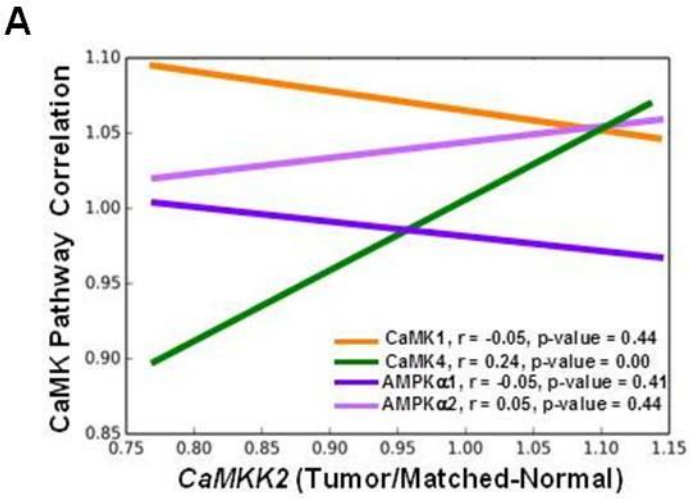

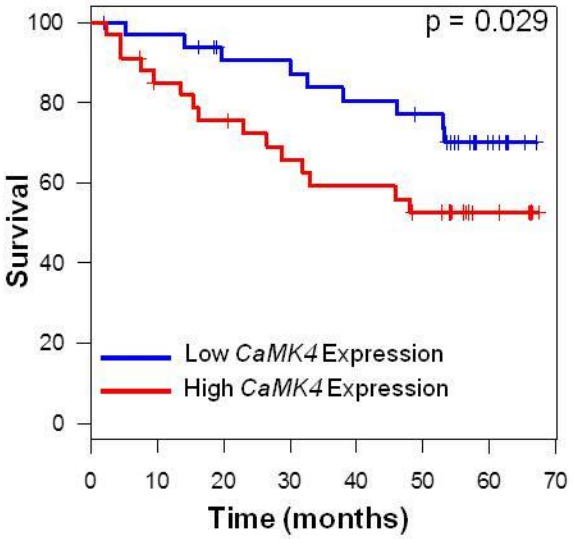

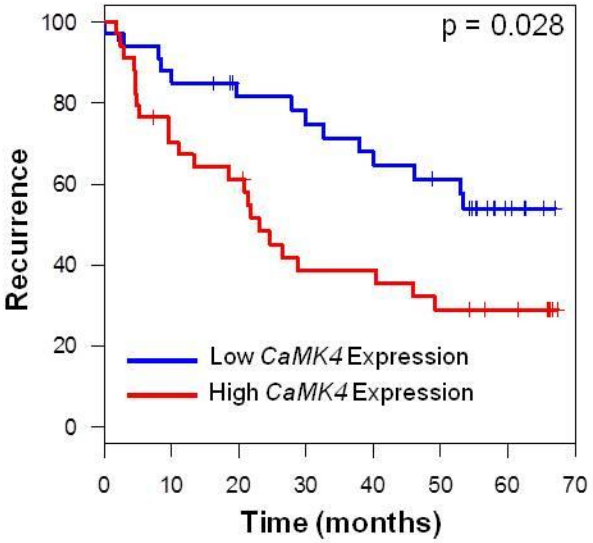

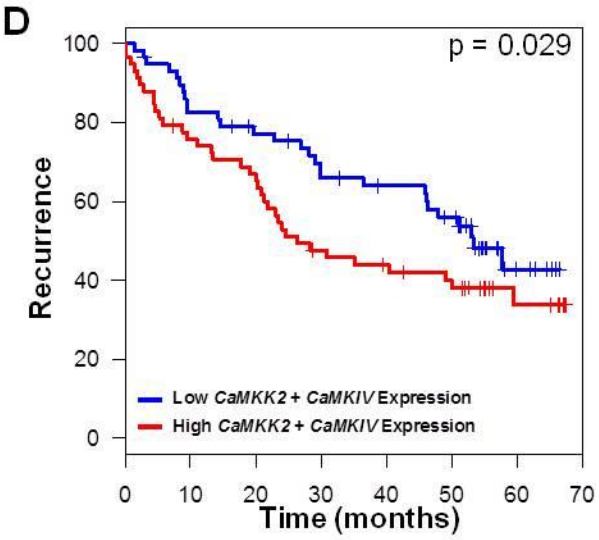

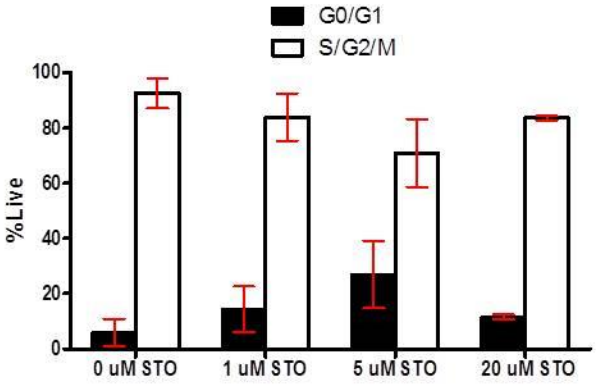

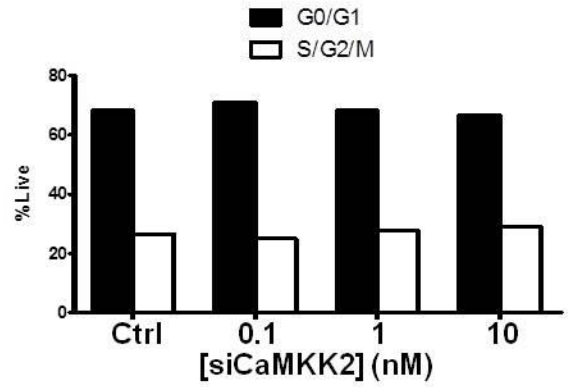

Supplemental Figure 3 - continued

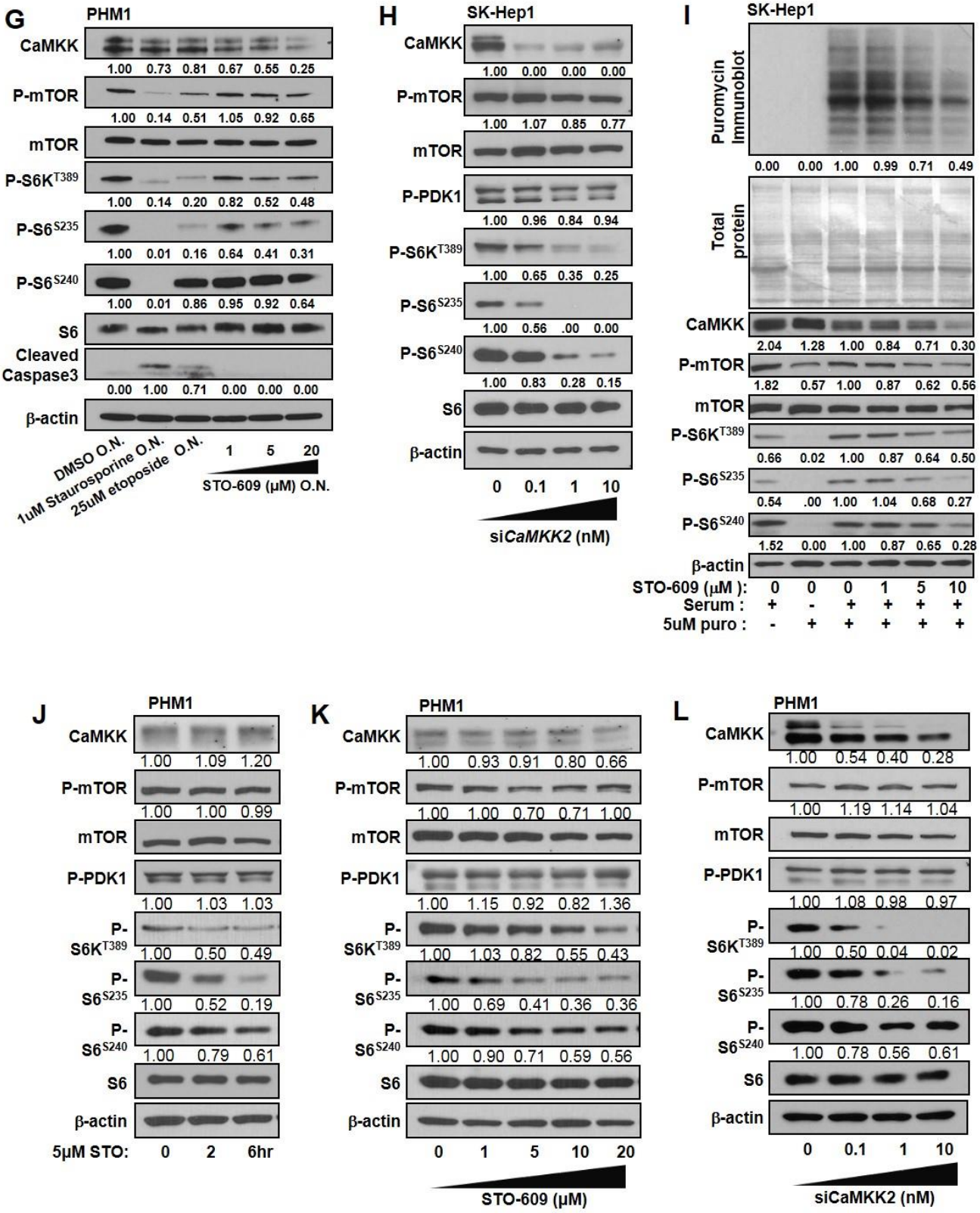

Supplemental Figure 3. Loss of CaMKK2 has minimal effects on cell cycle and apoptosis, but coordinates the regulation of protein synthesis.
(A) Pearson correlations of *CaMKK2* gene expression with that of *CaMK1*, *CaMK4*, *AMPKa1* and *AMPKa2* in the human HCC microarray dataset (Roessler et al). Only *CaMK4* positively and significantly correlated with *CaMKK2* expression (R = 0.24, p = 0.0002).
(B) Kaplan-Meier survival plot of liver cancer patients (n = 247) comparing low *CaMK4* expression (blue lines) with high *CaMK4* expression (red lines).
(C) Kaplan-Meier recurrence plot of liver cancer patients (n = 247) comparing low *CaMK4* expression (blue lines) with high *CaMK4* expression (red lines).
(D) Kaplan-Meier recurrence plot of liver cancer patients (n = 247) comparing low *CaMKK2* + *CaMK4* expression (blue lines) with high *CaMKK2* + *CaMK4* expression (red lines).
(E) Cell cycle analysis of PHM1 cells treated with increasing doses of STO-609 for 48 hrs (n = 3).
(F) Cell cycle analysis of PHM1 cells treated with increasing doses of *CaMKK2* siRNA.
(G) PHM1 cells were treated with increasing doses of STO-609 or apoptosis-inducing chemicals (i.e. staurosporine and etoposide). Analysis of apoptosis markers for cleaved caspase 3 and components of the mTOR/S6K pathway were examined by immunoblot.
(H) Immunoblot of CaMKK2 targets and components of the mTOR/S6K pathway, including P-PDK1 in SK-Hep1 cells transfected with increasing doses of CaMKK2 siRNA.
(I) SK-Hep1 cells were serum-fasted overnight and treated with increasing doses of STO-609. *De novo* protein synthesis was monitored by adding back 10% serum and 5 μM puromycin for 2 h. Immunoblot of puromycin incorporation and coomassie staining for total protein are represented.
(J) Immunoblot analysis of PHM1 cells for various components of mTOR/S6K pathway in response to treatment with 5μM STO-609 for 0, 2 or 6 h, respectively.
(K) Immunoblot analysis of PHM1 cells for various components of the mTOR/S6K pathway in response to increasing doses of STO-609 for 16 h.
(L) Immunoblot analysis of the mTOR/S6K pathway in PHM1 cells transfected with increasing doses of *CaMKK2* siRNA.

Supplemental Figure 4

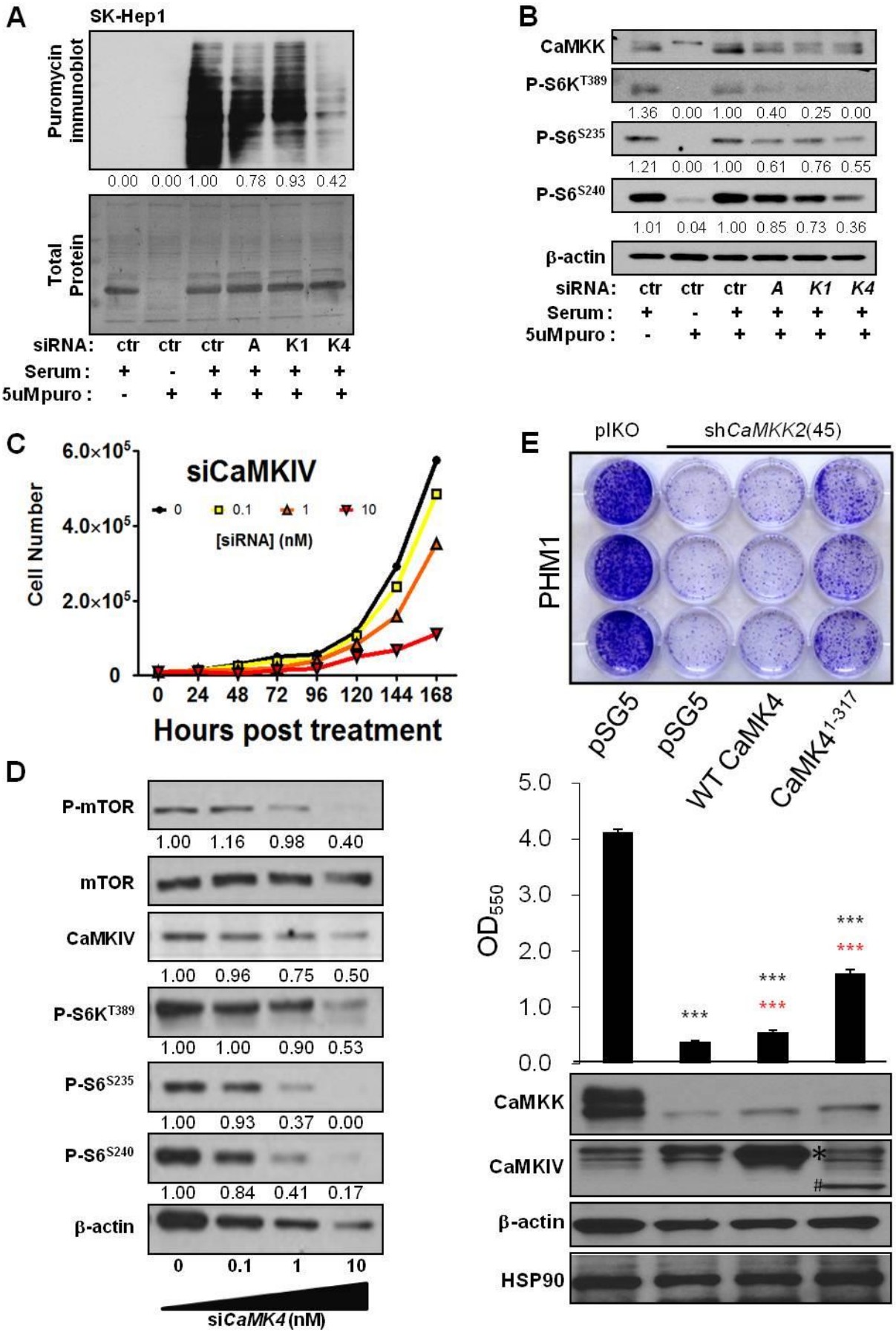

Supplemental Figure 4. CaMKK2 signals predominantly through CaMK4 to regulate liver cancer cell growth.

(A) SK-Hep1 cells were transfected with Control, *AMPK*α, *CaMK1* or *CaMK4* siRNA. Cells were serum-fasted overnight and *de novo* protein synthesis was monitored by adding back 10% serum and 5μM puromycin. Immunoblot of puromycin incorporation and coomassie staining for total protein are represented.

(B) Immunoblot analysis of protein knockdown from (A) and components of the mTOR/S6K pathway are shown.

(C) Time course proliferation assays of SK-Hep1 cells transfected with increasing doses of *CaMK4* siRNA.

(D) SK-Hep1 cells were transfected with increasing doses of *CaMK4* siRNA. Immunoblot analysis of CaMKIV and components of the mTOR/S6K pathway.

Data are graphed as the mean ± s.e.m. Shown are the representative replicates of at least three independent experiments. *p<0.05; **p<0.01, ***p<0.001.

(E) *Top panel*: crystal violet staining of colony formation assays of control and *CaMKK2*-null PHM1 cells transfected with indicated plasmids; *Middle panel*: Measurement of extracted crystal violet stain at O.D. 550 nm; *Bottom panel*: Immunoblot to verify the expression of CaMKK2 and CaMKIV. *p<0.05; **p<0.01, ***p<0.001. Black asterisk vs. plKO+pSG5; red asterisk vs. sh*CaMKK2*+pSG5. *: WT CaMKIV; #: CaMKIV$^{1\text{-}317}$.

Supplemental Figure 5

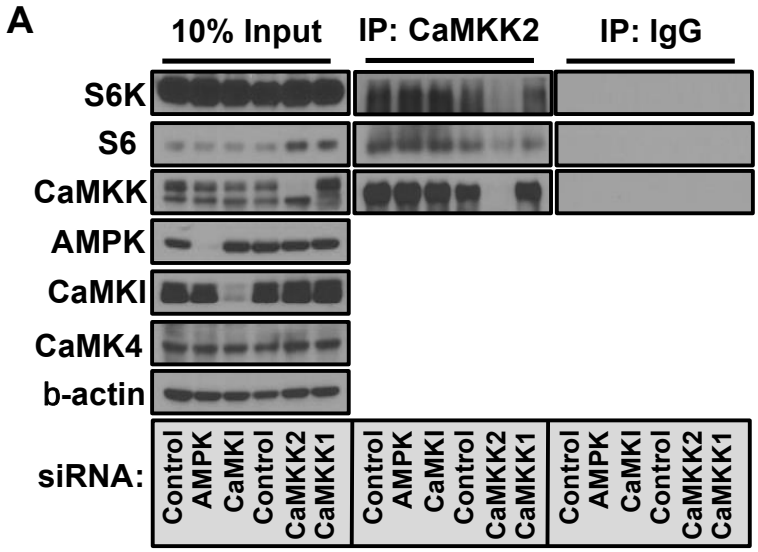

Supplemental Figure 5. CaMKK2 complexes with core components of the mTOR/S6K pathway.
(A) Immunoprecipitation with antibodies specific for CaMKK2 or mIgG from PHM1 cells treated with control siRNA, siRNAs specific for AMPK, CaMKI, CaMKK2 or CaMKK1, respectively. IP material was immunoblotted for components of the mTOR/S6K pathway as indicated. For all immunoprecipitations, 10% of input lysate used for each IP was immunoblotted as a loading control.

Supplemental Figure 6

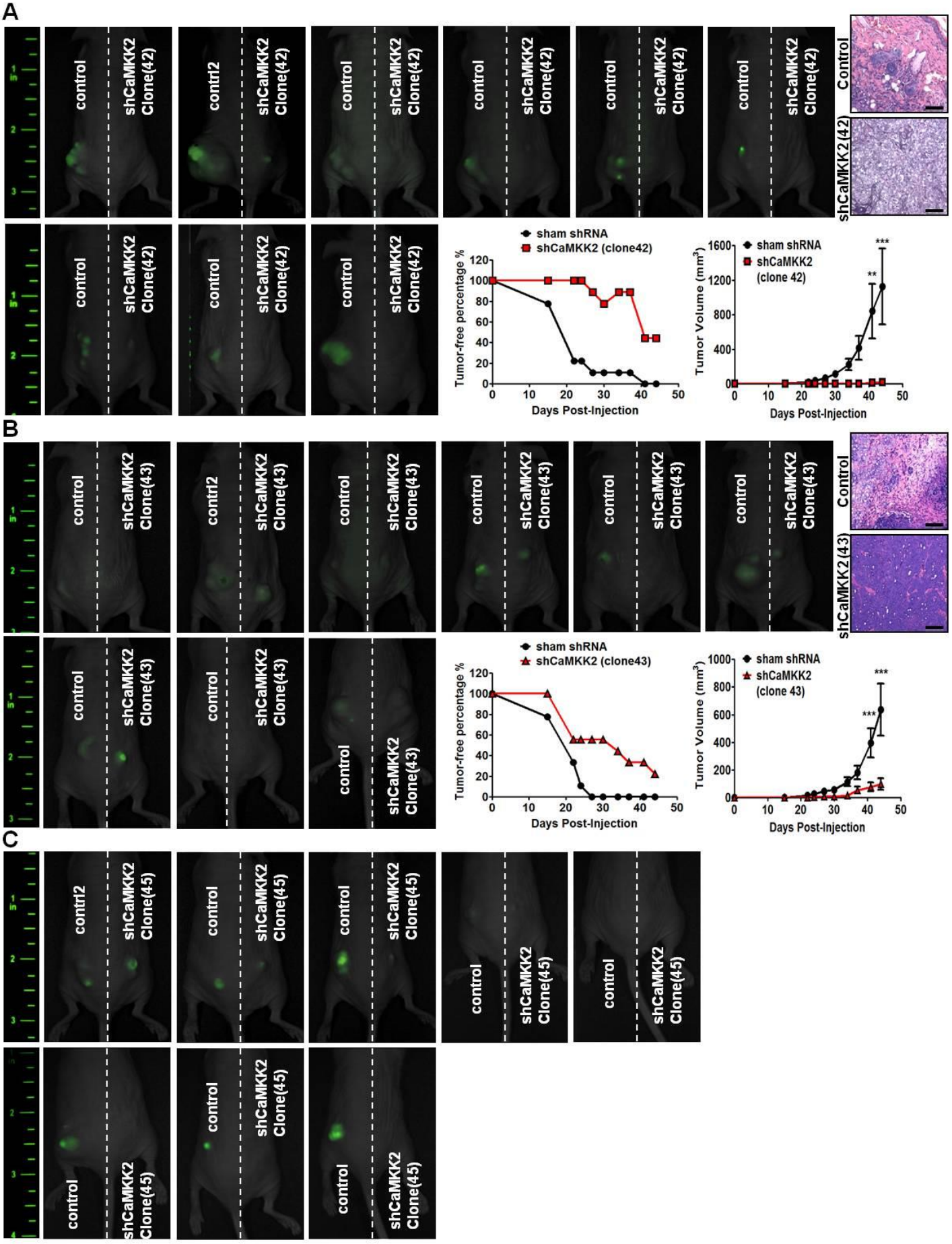

D

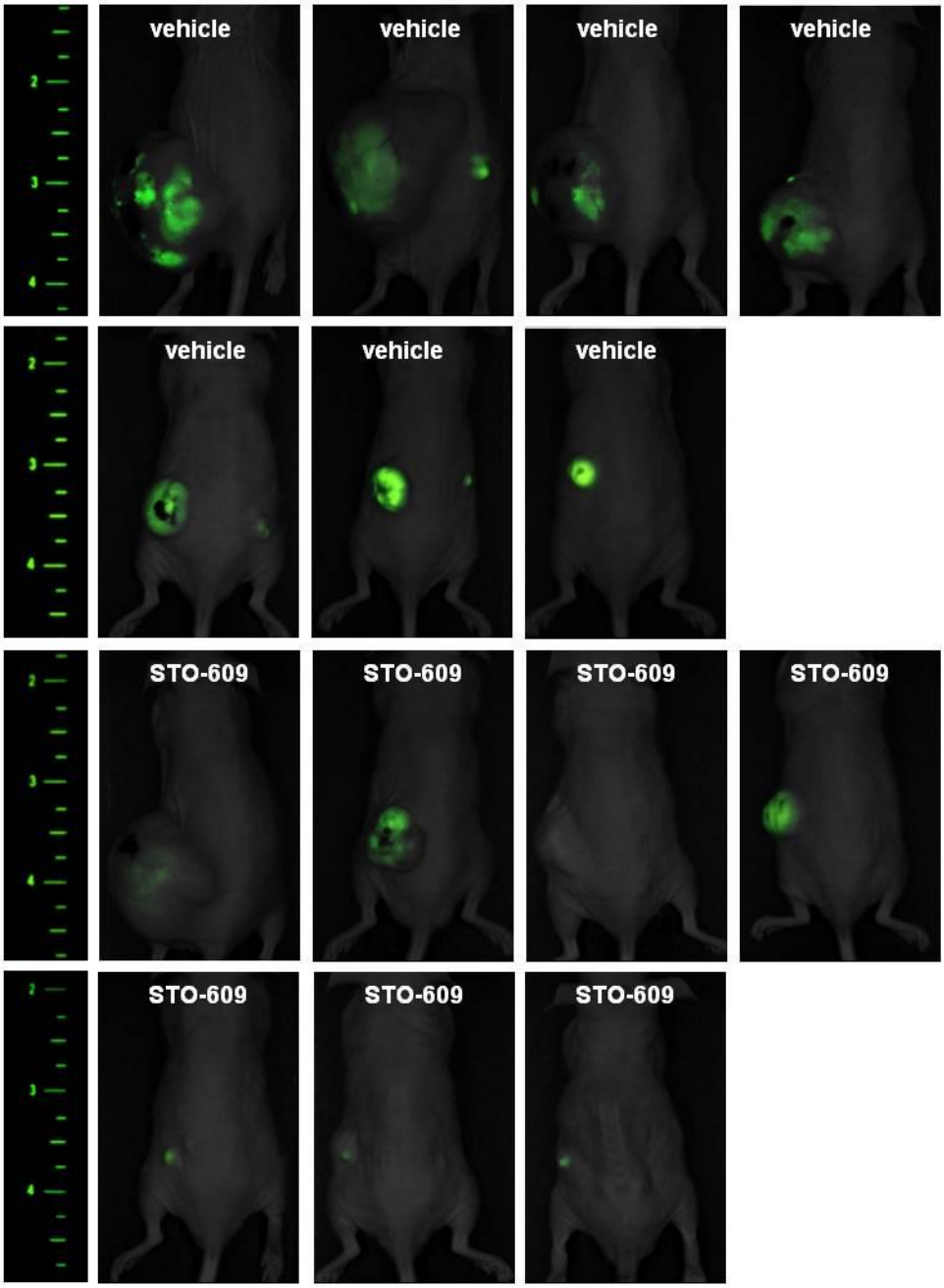

E

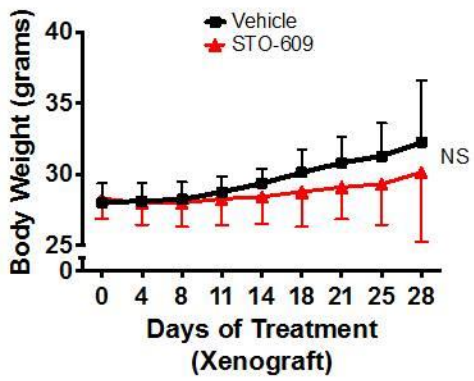

Supplemental Figure 6 - Continued

Supplemental Figure 6. Loss of CaMKK2 delays and attenuates PHM1 liver cancer cell outgrowth in nude mice.

(A) Longitudinal measurement of tumor outgrowth between control PHM1 cells versus PHM1 treated with sh*CaMKK2* (Clone ID: 3142). GFP fluorescence images of endpoint tumor outgrowth to detect tumors formed in nude mice. Tumor free percentage and quantification of the tumor volumes were determined over the study period. (n = 9). H & E stained paraffin-embedded sections of tumor biopsies from livers of nude mice injected with control PHM1 cells or sh*CaMKK2*-treated PHM1 cells. Scale bars = 20 μm.

(B) Longitudinal measurement of tumor outgrowth between control PHM1 cells versus PHM1 treated with sh*CaMKK2* (Clone ID: 3143). GFP fluorescence images of endpoint tumor outgrowth to detect tumors formed in nude mice. Tumor free percentage and quantification of the tumor volumes were determined over the study period. (n = 9). H & E stained paraffin-embedded sections of tumor biopsies from livers of nude mice injected with control PHM1 cells or shCaMKK2-treated PHM1 cells. Scale bars = 20 μm.

(C) Longitudinal measurement of tumor outgrowth between control PHM1 cells versus PHM1 treated with sh*CaMKK2* (Clone ID: 3145). GFP fluorescence images of endpoint tumor outgrowth to detect tumors formed in nude mice. Tumor free percentage and quantification of the tumor volumes were determined over the study period. (n = 9). H & E stained paraffin-embedded sections of tumor biopsies from livers of nude mice injected with control PHM1 cells or sh*CaMKK2*-treated PHM1 cells. Scale bars = 20 μm.

(D) Control PHM1 cells (2 x 10^6/100μL) were subcutaneously injected into nude mice and tumor volume was allowed to develop to 3mm3. Tumor bearing mice were i.p. injected with either vehicle (10% DMSO in PBS) or STO-609 (30 μg/kg body weight) 2X/week for four weeks (n = 8/treatment group). Shown is GFP fluorescence images of endpoint tumor outgrowth. Data are graphed as the mean ± s.e.m. **p<0.01, ***p<0.001.

(E) Periodic body weight measurements of WT mice from Figure 6C injected with either vehicle (10% DMSO in PBS) or STO-609 (30μg/kg body weight) 2X/week for four weeks.

Supplemental Figure 7

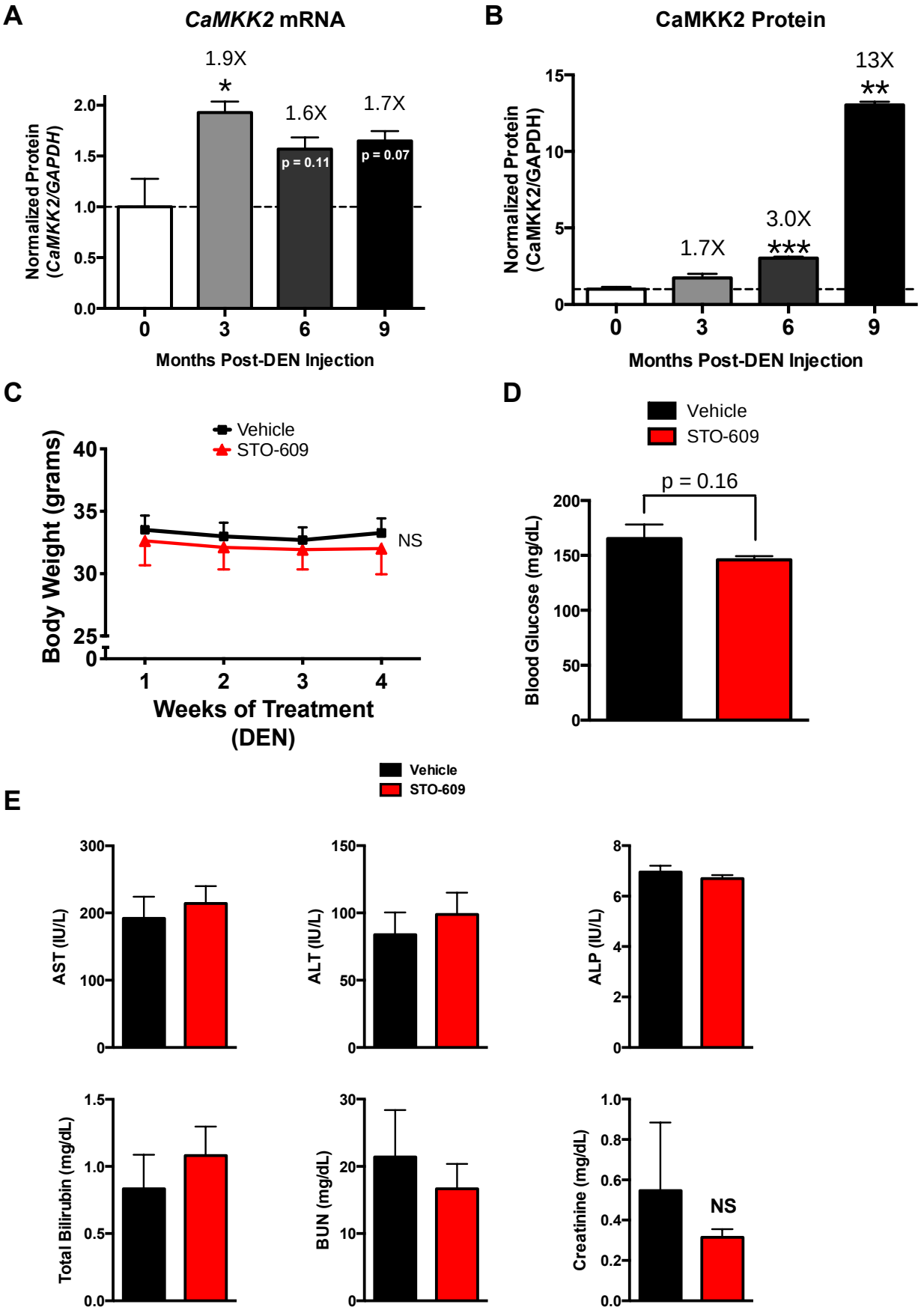

F

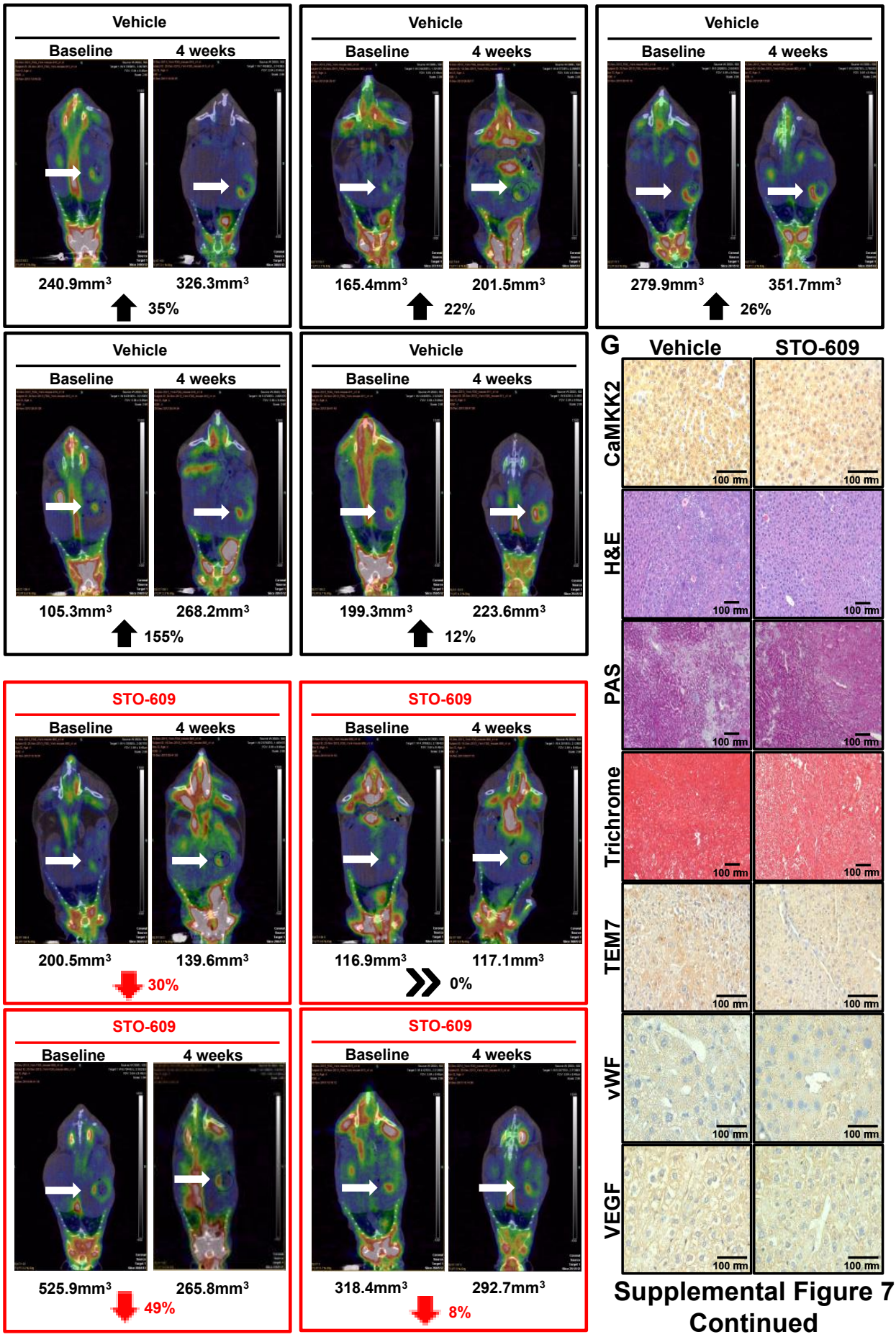

G

Supplemental Figure 7
Continued

Supplemental Figure 7. Loss of CaMKK2 renders beneficial effects on DEN-induced hepatic tumorigenesis.
(A) qPCR analysis of normalized *CaMKK2* mRNA in liver samples of WT mice 0, 3, 6 and 9 months post-DEN injection.
(B) Quantitation of CaMKK2 immunoblot densitometry from Figure 7B.
(C) Weekly body weight measurements of WT mice from Figure 7C treated with either vehicle (10% DMSO in PBS) or STO-609 (30µg/kg body weight) 2X/week for four weeks.
(D) Measurement of terminal blood glucose of WT mice from Figure 7C treated with either vehicle (10% DMSO in PBS) or STO-609 (30µg/kg body weight) 2X/week for four weeks.
(E) Hepatic (ALT, AST, ALP), renal (BUN, creatinine) and hematological (total bilirubin) analysis of plasma samples from WT mice from Figure 7C treated with either vehicle (10% DMSO in PBS) or STO-609 (30µg/kg body weight) 2X/week for four weeks.
(F) WT mice were injected with DEN. Six months post-injection, mice were monitored by PET/CT imaging to establish a baseline tumor burden. Tumor bearing mice were i.p. injected with either vehicle (10% DMSO in PBS) or STO-609 (30µg/kg body weight) 2X/week for four weeks. After four weeks, mice were monitored again by PET/CT imaging to quantify changes in tumor burden. Quantitation of tumor volume is listed at baseline and following the four week treatment. Comparison of % change of the tumor burden between vehicle and STO-609 treatment groups is listed.
(G) Histological (H&E, Periodic Acid-Schiff staining (PAS), Trichrome) and immunohistological (CaMKK2, von Willebrand Factor (vWF), Tumor Endothelial Marker (TEM7), Vascular Endothelial Growth Factor (VEGF)) analysis of WT livers from vehicle and STO-609 treated mice from Figure 7C.